forests

MDPI

Article

Prediction of Hazard Trees Based on Functional Groups, Succession, and Climate Zones

Ming-Hsun Chan, Pei-Ju Chen and Jung-Tai Lee *

Department of Forestry and Natural Resources, College of Agriculture, National Chiayi University, Chiayi City 60004, Taiwan; mhchan@mail.ncyu.edu.tw (M.-H.C.); s1140006@mail.ncyu.edu.tw (P.-J.C.)
* Correspondence: jtlee@mail.ncyu.edu.tw

Abstract

Despite five years of hazard tree investigation and mitigation (Potential Hazard Tree monitoring and hazard tree removal) from 2020 to 2024, the incidence ratios of hazard trees (HTs) and Potential Hazard Trees (PHTs) along the Alishan Forest Railway corridor (spanning subtropical, warm temperate, and temperate zones) have not exhibited a significant downward trend. This study aims to investigate the impacts of climate zones, succession, and functional groups on hazard tree occurrence and to further predict the incidence ratios of hazard trees. We employed Generalized Linear Models (GLMs) and structural defect frequency to evaluate these interactions. The significance of the impacts is ranked as follows: functional group > succession regeneration > climate zone. Incidence was highest in subtropical (S) and warm temperate (W) zones (S ≈ W > T), and significantly greater for secondary succession (SS) areas compared to Planning Plantation (PP). Crucially, heliophilous species (H + P; small-to-medium pioneer and canopy heliophilous species) contributed significantly more to hazard incidence than non-heliophilous species (MT + T; mid-shade-tolerant and shade-tolerant species). Model predictions identified (H + P) + SS + S as the highest-incidence ecological combination, while (MT + T) + PP + T was the lowest. Structural defect relative frequency analysis revealed that the fast-growth strategy of H + P species fundamentally compromises their biomechanical stability, resulting in significantly higher defect frequencies compared to MT + T species. Furthermore, continuous corridor disturbances maintain a persistent light environment that perpetually recruits these H + P species via secondary succession. To effectively manage the incidence of HT and PHT, future mitigation measures must prioritize Planning Plantation (PP) using non-heliophilous (MT + T) species selected within their appropriate ecological amplitudes.

Keywords: climate zone; Succession Regeneration; functional group; tree failure assessment

Check for updates

Academic Editor: Giorgos Mallinis

Received: 4 February 2026
Revised: 6 March 2026
Accepted: 10 March 2026
Published: 24 March 2026

Copyright: © 2026 by the authors. Licensee MDPI, Basel, Switzerland. This article is an open access article distributed under the terms and conditions of the Creative Commons Attribution (CC BY) license.

1. Introduction

1.1. Tree Failure Hazard Railway Safety

The Alishan Forest Railway corridor, spanning 85 km in length, vertically traverses subtropical, warm temperate, and temperate climate zones. Operational since 1912, the railway initially focused on timber extraction before introducing passenger services in 1920, marking a 106-year operational history. However, this unique mountain railway environment poses severe challenges for infrastructure management. On 27 April 2011, a major hazard tree failure occurred along the corridor. The phototropic growth of a *Quercus morii* led to the over-extension of its scaffold branches; the subsequent fracture of co-dominant stems struck a moving train carriage, resulting in five fatalities and 113 injuries [1].

Despite ongoing hazard tree identification and management efforts, the frequency of tree failures has not decreased, posing a persistent threat to the operational safety of the railway.

1.2. Hazard Tree Identification

Hazard tree identification is based on the ANSI A300 (Part 9) tree risk assessment standards established by the Tree Care Industry Association [2]. Following the USDA Forest Service definition of the Potential Impact Zone (PIZ), trees possessing failure potential capable of causing damage along the railway corridor are classified as Target Trees. Specifically, trees with a diameter at breast height (DBH) greater than 10 cm, whose PIZ (defined as 1.5 times the tree height) overlaps with the safe operational zone, are designated as Candidate Investigation and Assessment Trees (CIAT) [3].

CIATs are evaluated using a Health/Hazard Tree Identification (HHTI) rating system (scored 1–16). This rating is derived by multiplying a biological vitality score [4] by a structural failure potential score [5–7]. Vitality is categorized into four levels based on morphology: 1 (good/vigorous), 2 (fair), 3 (weak/declining), and 4 (decline/nearing death). Similarly, failure potential is divided into four levels based on structural defects: 1 (none), 2 (low/minor defects), 3 (moderate/residual wood approaching minimum limits), and 4 (high/significant defects or dead trees). Based on the multiplied HHTI scores, CIATs are stratified into three management categories:

Safe Tree (ST; score $\leq$ 2): None to low failure potential. These trees exhibit strong structural and biological integrity, posing no threat.

Potential Hazard Tree (PHT; score 3–6): Low to moderate failure potential. These individuals possess minor to moderate defects requiring Level 3 Advanced Assessment or monitoring, as environmental stress may escalate their failure potential.

Hazard Tree (HT; score $\geq$ 8): Moderate to high failure potential. These trees display significant defects, constituting an immediate threat to railway operational safety requiring prompt mitigation.

While these existing frameworks systematically quantify visual defects, they primarily focus on assessing current health status and biomechanical symptoms. However, the functional traits of tree species result in varying levels of tolerance and resistance to health or structural defects, leading to divergent outcomes in tree failure and collapse [8–10].

1.3. Climate and Vegetation Zones with Succession

The winding railway corridor spans a 2000 m elevational gradient (from 50 m to 2600 m). Forest vegetation exhibits distinct vertical zonation, ranging from high-diversity subtropical broadleaf forests and warm temperate mixed needle–broadleaf forests to structurally simple temperate coniferous forests [11–14]. Forest structure and composition are governed by a dynamic mechanism shaped by disturbance, succession, and regeneration [15]. Forest succession can be categorized into four primary stages.

Stand Initiation Phase: Open or newly disturbed lands are colonized and developed by fast-growing pioneer (P) or heliophilous (H) species.

Stem Exclusion Phase: As the stand approaches canopy closure and resource saturation, tall and competitive heliophilous (H) trees become dominant, outcompeting weaker individuals through light and space competition.

Understory Reinitiation Phase: Gaps appear in the aging forest canopy, increasing light availability; mid-tolerant (MT) or shade-tolerant (T) species begin to recruit and develop in the understory.

Climax Phase: The forest structure reaches a dynamic equilibrium, dominated by long-lived, shade-tolerant (T) species characterized by high structural stability, forming a stable self-regeneration cycle [16].

The railway corridor is frequently subjected to continuous light exposure and slope erosion, which triggers secondary succession (SS) [16]. In contrast to the natural dynamics of SS, Planning Plantation (PP)—primarily found in warm temperate and temperate zones—consists of managed coniferous forests that exhibit high structural homogeneity due to silvicultural objectives [17,18]. The successional pathway (SS vs. PP) determines the composition of plant functional groups [19], which in turn exhibit divergent growth and resource allocation strategies [8–10]. These successional mechanisms drive the differentiation of functional groups; the resulting disparities in stress tolerance and structural stability constitute the core complexity of hazard tree management.

1.4. Aim of the Investigation

Our five-year hazard tree survey and mitigation operations (2020–2024) demonstrate that, despite persistent intervention, the incidence ratios of hazard trees (HTs) and Potential Hazard Trees (PHTs) have not decreased to an acceptable safety threshold (Figure 1). Current mitigation strategies—strictly adhering to ANSI A300 and USDA Forest Service standards, trigger removal once the Health/Hazard Tree Identification (HHTI) rating score reaches the hazard tree. However, this diagnostic approach fails to account for tree functional traits, successional regeneration status, and climate zones. Consequently, a critical inconsistency persists: trees with identical structural defect scores exhibit divergent stability, where certain species remain standing while others suffer catastrophic failure.

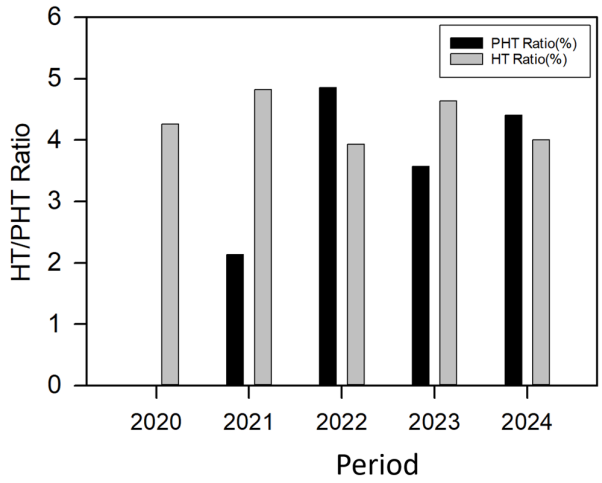


Figure 1. Incidence of HT/PHT during the five-year period from 2020 to 2024 (source: original field survey conducted for this study).

Leveraging the complete elevational gradient and rich taxonomic diversity of the Alishan mountain range, this study aims to elucidate the roles that climate-driven vegetation zones, functional traits, and successional regeneration patterns play in the occurrence of hazard trees along the railway corridor. We seek to determine the relative influence weights of these ecological factors on hazard incidence ratios. Ultimately, this research provides a scientific reference for species-specific management and forest regeneration strategies along the elevational gradient, ensuring that railway safety management remains within an acceptable range.

2. Materials and Methods

2.1. Study Area

The railway is situated within the Alishan mountain range, ascending from the western plains at an elevation of approximately 50 m to mountainous areas at nearly 2600 m. This steep elevational gradient divides the corridor into three distinct climate zones. The

subtropical (S) zone, located at elevations of 50–997 m, is characterized by a high mean annual temperature (18–24 °C) and an annual precipitation of approximately 2000–2500 mm. The warm temperate (W) zone, spanning elevations from 997 to 1711 m, features moderate temperatures (13–18 °C) and an annual precipitation of roughly 3000–3500 mm. Finally, the temperate (T) zone, ranging from 1711 to 2405 m, is characterized by a cool environment with a mean annual temperature of 10–12 °C and an annual precipitation of approximately 3500–4000 mm [11,12] (Figure 2).

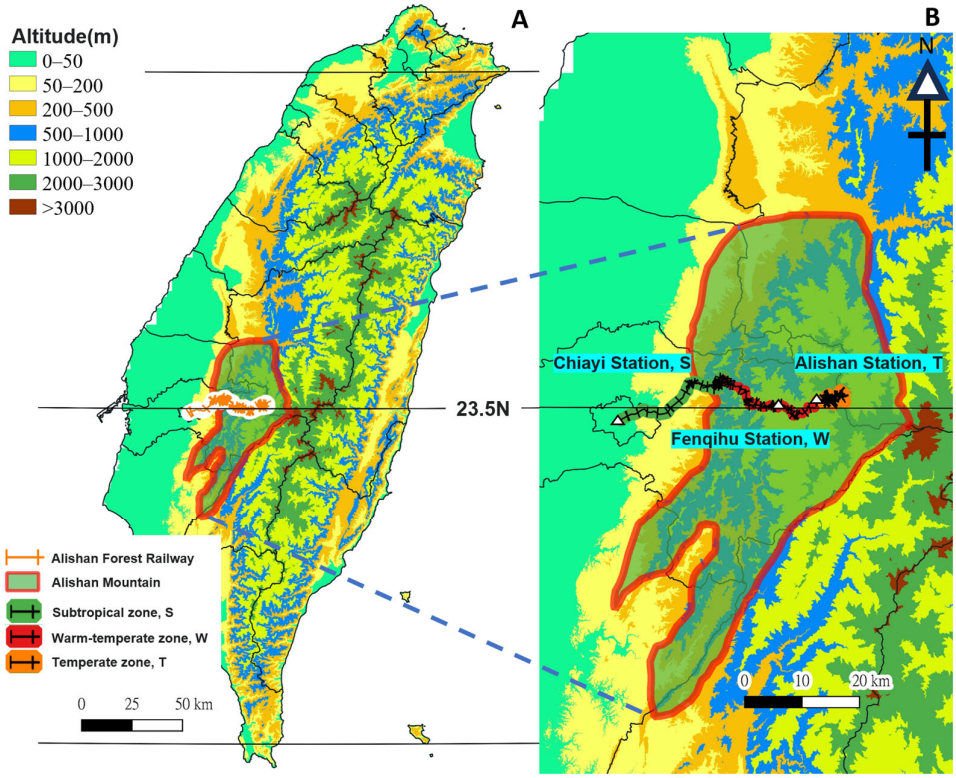


Figure 2. Geographical location and climatic zone of the study area. (**A**) Topographic map of Taiwan, including the location of the Alishan Mountain range and the overall route of the Alishan Forest Railway along the elevational gradient. (**B**) Detailed map of the railway corridor, the spatial distribution of the three climatic zones: subtropical zone (S, starting near Chiayi Station), warm temperate zone (W, passing through Fenqihu Station), and temperate zone (T, terminating at Alishan Station). Software: QGIS (version 3.28, QGIS Association, Gossau, Switzerland). Data Source: Ministry of the Interior, Taipei, Taiwan.

2.2. Materials

2.2.1. Candidate Investigation and Assessment Tree (CIAT) Survey

All Candidate Investigation and Assessment Trees (CIATs) were surveyed to document species identification and tree geometric characteristics, specifically diameter at breast height (DBH) and tree height. The Importance Value Index (IVI) was calculated as the sum of relative density, relative frequency (RF), and relative dominance (RDo). RF was determined based on species distribution across different altitudinal zones, while RDo was derived from the basal area calculated using DBH data [20]. The structural complexity of the forest communities was quantified using the Shannon diversity index (H′) and Simpson's dominance index (λ). These indices were subsequently converted into Hill numbers (N1 and N2), representing the effective number of "abundant species" and "very abundant species," respectively. Finally, the modified Hill ratio (E5) was employed to calculate community evenness [21–24].

2.2.2. Hazard Tree Identification

This study adopted the hazard tree scoring system from the United States Department of Agriculture (USDA) guidelines, Hazard Tree Identification and Mitigation. Since the study area is restricted to the railway corridor, a high target value (encompassing tracks, facilities, and personnel) is consistently applied. Hazard trees are evaluated using the Visual Tree Assessment (VTA) [25] to determine physiological condition and mechanical structural stability based on biological vitality and structural defects.

The Health Vitality Assessment followed the International Society of Arboriculture (ISA) Guide for Plant Appraisal, 10th Edition [4]. Tree health vitality was rated on a scale of 1 to 4 (1: good; 2: fair; 3: weak; 4: decline). The assessment evaluated five indicators: (1) crown density, (2) foliage characteristics (color and size), (3) live crown ratio, (4) dieback, and (5) shoot growth over the past three years.

The Structural Defect Assessment utilized the USDA guideline Hazard Tree Identification and Mitigation [3,26–33]. Defect severity was rated on a scale of 1 to 4 (1: no defect/no failure potential; 2: minor defect/low failure potential; 3: moderate defect/moderate failure potential; 4: severe defect/high failure potential). Scoring was based on the single most severe defect present; if multiple interacting defects existed, the score of the most severe defect was incremented by 1 (up to a maximum of 4). Dead trees were automatically rated as 4. The inspection covers nine indicators across five primary categories: whole tree structure: D1 = lean; root structure: D2 = root decay, D3 = root structural defects, and D4 = root plate soil separation; trunk base: D5 = trunk base decay; scaffold branches: D6 = over-extended branches, D7 = co-dominant stems, and D8 = scaffold branch decay; and overall physiological state: D9 = growth decline or deadwood.

2.3. Methodology

2.3.1. Hazard Tree (HT) and Potential Hazard Tree (PHT) Incidence Ratio

Railway corridor spans three climate zones and contains numerous species; however, species population distribution is uneven, where specific populations (*Chamaecyparis formosensis*, *Cryptomeria japonica*) vastly outnumber others. Analysis utilizing raw HT or PHT counts would induce severe bias from these unbalanced sample sizes, disproportionately amplifying the attribute of dominant species. The standardized incidence ratio was, therefore, adopted as the analytical basis to eliminate this sampling bias. *HT* and *PHT ratios* for each species are calculated as follows.

$$HT\ Ratio = HT/CIAT \times 100 \quad (1)$$

$$PHT\ Ratio = PHT/CIAT \times 100 \quad (2)$$

2.3.2. Functional Group

Tree species are categorized into four basic types—pioneer (P)—small-to-medium heliophilous species; heliophilous (H)—heliophilous canopy species; mid-shade-tolerant (MT)—mid-shade-tolerant emergent canopy species; shade-tolerant (T)—medium shade-tolerant species—based on phototaxis, growth rate, resource allocation, and wood density [8,9,34]. Two primary analytical functional groups were further consolidated—heliophilous and non-heliophilous groups [10]. The heliophilous group (H + P) comprises H (heliophilous) and P (pioneer) species. The non-heliophilous group (MT + T) comprises MT (mid-shade-tolerant) and T (shade-tolerant) species (Table 1).

Table 1. Dependent variables—HT/PHT. Independent variables: functional group + succession regeneration + climate zone (FSC).

Variable	Definition	Mean/Count
Hazard Tree Ratio, HT (%)	Ratio of trees with moderate-to-high failure potential	9.96
Potential Hazard Tree Ratio, PHT (%)	Ratio of trees with low-to-moderate failure potential	9.20
Functional Group	H + P = heliophilous	N = 548
	MT + T = non-heliophilous	N = 2775
Succession Regeneration	SS = secondary succession	N = 694
	PP = planning plantation	N = 2629
Climate Zone	S = subtropical zone	N = 380
	W = warm temperate zone	N = 1109
	T = temperate zone	N = 1834

2.3.3. Succession Regeneration

During the identification of hazard trees, each individual was simultaneously categorized as originating from secondary succession (SS) [16] or Planning Plantation (PP) [35] (Tables 1 and 2).

Table 2. Tree species diversity across climate zones. The subtropical (S) and warm temperate (W) zones exhibit higher species diversity (S: 55; W: 72). S = subtropical zone, W = warm temperate zone, T = temperate zone.

Climate Zone	Species	λ	H′	N1	N2	E5
S	55	0.06	3.31	27.32	17.30	0.62
W	72	0.47	1.87	6.49	2.11	0.20
T	17	0.57	0.88	2.40	1.77	0.55

2.3.4. Statistical Analysis

Correlation Analysis

Pearson's product–moment correlation was employed to examine the linear relationship between hazard trees (HTs) and Potential Hazard Trees (PHTs). The analysis utilized a two-sided test with a significance level ($\alpha = 0.05$). The null hypothesis posits no linear association between the variables ($\rho = 0$), while the alternative hypothesis asserts the existence of a linear association ($\rho \neq 0$).

Model Construction

The Generalized Linear Model (GLM) was utilized to analyze and predict the influence of various factors on hazard trees (HTs) and Potential Hazard Trees (PHTs) [36,37]. Models for HT and PHT incidence ratios were constructed using 2020–2024 railway corridor survey data, incorporating functional group, succession regeneration, and climate zone as variables. The Poisson distribution was selected to model the frequency of event occurrences within specific intervals. A log link function was employed as the canonical link function to ensure strictly positive predicted incidence ratios [38].

$$\log(HT\ Ratio) = a + b1(fuctional\ group) + b2(Succession\ Regeneration) + b3(climate\ zone) \quad (3)$$

$$\log(PHT\ Ratio) = a + b1(fuctional\ group) + b2(Succession\ Regeneration) + b3(climate\ zone) \quad (4)$$

The GLM model output includes the following metrics:

Estimate—the raw coefficient calculated by the model on a log-scale.

Standard error—represents the uncertainty associated with the estimate.

p-value—indicates statistical significance, determining the significance of the specific factor.

Exponentiated coefficients—(exp (estimate)) represent the incidence ratio. This metric is used to quantify the influence of each factor on the HT or PHT incidence ratio relative to the reference group.

Model Prediction

The statistical significance of factors within the GLM confirmed the model's predictive capability. To further quantify incidence differences across various factor combinations, the established model was employed to predict and compare the HT and PHT incidence ratios for all 12 variable combinations of functional group, succession regeneration, and climate zone (FSC). Subsequently, a one-sample *t*-test was conducted on the predicted incidence ratio across all 12 scenarios to verify the overall significance of their distribution.

Structural Defects Relative Frequency Analysis

One-way ANOVA was employed to analyze defect type frequency distributions within HT and PHT populations, utilizing functional group as the factor to detect significant differences in structural defect occurrences. Defect frequency calculation normalized the data to eliminate population size bias by dividing specific defect counts (D1–D9) by the population of each respective functional group (H + P, n = 548, MT + T, n = 2775).

$$\text{Defects Frequency}(\%) = \left(\frac{\text{Defect count}(D1 - D9)}{\text{Tree population of respective Functional Group}(n)} \right) * 100 \quad (5)$$

3. Results

3.1. Tree Species Composition, Structure, and Hazard Trees by Climate Zone

3.1.1. Tree Species Composition and Structure

The vegetation composition along the railway corridor comprises 110 species across 45 families. The subtropical (S) zone exhibited the highest Shannon diversity index ($H' = 3.31$) and high evenness (E5 = 0.62), indicating a relatively balanced resource distribution among its 55 species. This zone is characterized by high-diversity broadleaf forests with extremely low community dominance ($\lambda = 0.06$), where no single species exerts absolute dominance. The community primarily consists of the shade-tolerant (T) species *Dimocarpus longan* (IVI = 4.43) and several heliophilous (H) species with IVI values ranging between 1.0 and 2.0, including *Tabebuia impetiginosa*, *Spathodea campanulata*, *Koelreuteria henryi*, and *Bombax ceiba*. The warm temperate (W) zone displayed the highest species richness (73 species). However, its community structure is dominated by a few abundant species, characterized by high dominance ($\lambda = 0.47$) and low evenness (E5 = 0.20). The broadleaf layer in this zone comprises *Trema orientalis*, IVI = 9.91 (H), *Heptapleurum heptaphyllum*, IVI = 6.47 (T), *Machilus zuihoensis*, IVI = 5.45 (MT), and *Mallotus paniculatus*, IVI = 4.00 (P). The coniferous layer is influenced by Planning Plantation (PP) and shows a transition toward managed forest structures, primarily consisting of *Cryptomeria japonica*, *Chamaecyparis formosensis*, and *Cunninghamia konishii*. The temperate (T) zone possesses a relatively simple vegetation structure, with most areas categorized as Planning Plantation (PP), resulting in the lowest species richness (17 species). Its diversity ($H' = 0.88$) and dominance ($\lambda = 0.57$) indices reflect an environment dominated by a few ubiquitous species. The community is predominantly composed of *Cryptomeria japonica*, IVI = 116.13, and *Chamaecyparis formosensis*, IVI = 21.86. The high IVI values of these species correspond with the high community dominance, highlighting the structural homogeneity characteristic of managed forest plantations (Tables 2 and 3).

Table 3. Railway Corridor Candidate Inventory and Assessment Tree (CIAT), hazard tree (HT), Potential Hazard Tree (PHT), scientific name, functional group (P, H, MT, T), succession regeneration (SS, PP), climate zone (S, W, T), 2020 count, 2024 count, and Importance Value Index (IVI). Species are sorted first by elevational gradient (from low to high elevation) and subsequently by their IVI in descending order within each zone. Data were obtained from our field surveys.

Species Name	Family	Functional Group	SS/PP	HT	PHT	N20	N24	S	W	T	IVI
Dimocarpus longan	Sapindaceae	T	SS	10	8	39	37	-			4.43
Tabebuia impetiginosa	Bignoniaceae	H	PP	6	0	17	11	-			1.89
Spathodea campanulata	Bignoniaceae	H	SS	9	10	6	7	-			1.75
Koelreuteria henryi	Sapindaceae	H	SS	8	3	10	5	-			1.65
Bombax ceiba	Malvaceae	H	PP	1	1	2	2	-			1.27
Alstonia scholaris	Apocynaceae	MT	PP	0	0	10	10	-			1.12
Sterculia monosperma	Malvaceae	H	SS	0	9	0	9	-			1.08
Jacaranda acutifolia	Bignoniaceae	H	PP	2	2	3	3	-			0.87
Phoebe formosana	Lauraceae	MT	SS	0	1	1	2	-			0.84
Swietenia mahagoni	Meliaceae	MT	PP	0	0	6	6	-			0.79
Cassia fistula	Fabaceae	MT	PP	0	0	6	6	-			0.70
Tectona grandis	Lamiaceae	MT	PP	0	0	2	2	-			0.63
Senna siamea	Fabaceae	H	PP	1	3	2	4	-			0.63
Ficus ampelos	Moraceae	H	SS	0	1	2	3	-			0.56
Bauhinia variegata	Fabaceae	P	SS	0	1	1	2	-			0.51
Bauhinia purpurea	Fabaceae	P	SS	2	4	0	2	-			0.49
Melia azedarach	Meliaceae	H	SS	1	1	2	2	-			0.48
Mangifera indica	Anacardiaceae	T	PP	0	0	2	2	-			0.47
Cordia aspera	Cordiaceae	T	SS	1	0	2	1	-			0.46
Ficus superba var. *japonica*	Moraceae	H	SS	0	1	0	1	-			0.44
Terminalia mantaly	Combretaceae	MT	PP	0	0	1	1	-			0.43
Erythrina crista-galli	Fabaceae	H	SS	0	1	0	1	-			0.43
Bauhinia × *blakeana*	Fabaceae	P	SS	1	0	1	0	-			0.43
Rhus succedanea	Anacardiaceae	H	SS	1	1	0	0	-			0.43
Cocos nucifera	Arecaceae	MT	PP	0	0	1	1	-			0.42
Ficus virgata	Moraceae	H	SS	0	1	0	1	-			0.42
Neolitsea aciculata var. *variabillima*	Lauraceae	T	SS	0	0	2	2	-			0.42
Helicia formosana	Proteaceae	T	SS	0	0	1	1	-			0.41
Ziziphus dulcis	Rhamnaceae	H	SS	1	1	0	0	-			0.41
Ficus septica	Moraceae	H	SS	0	1	0	1	-			0.41
Neolitsea konishii	Lauraceae	MT	SS	0	0	1	1	-			0.41
Pittosporum pentandrum	Pittosporaceae	T	SS	0	1	0	1	-			0.41
Machilus philippinensis	Lauraceae	MT	SS	0	0	1	1	-			0.4
Trema orientalis	Cannabaceae	H	SS	61	63	55	57	-	-		9.91
Heptapleurum heptaphyllum	Araliaceae	T	SS	5	7	40	42	-	-		6.47
Machilus zuihoensis	Lauraceae	MT	SS	4	4	24	24	-	-		5.45
Mallotus paniculatus	Euphorbiaceae	P	SS	20	43	3	26	-	-		4.00
Acacia confusa	Fabaceae	H	SS	25	25	11	11	-	-		3.84
Camphora officinarum	Lauraceae	MT	PP	5	12	10	17	-	-		3.68
Ficus irisana	Moraceae	H	SS	2	14	0	12	-	-		2.62
Elaeocarpus decipiens	Elaeocarpaceae	H	SS	3	12	3	12	-	-		2.42
Macaranga tanarius	Euphorbiaceae	P	SS	13	14	5	6	-	-		2.38
Polyspora axillaris	Theaceae	T	SS	0	2	4	6	-	-		2.01
Machilus japonica var. *kusanoi*	Lauraceae	MT	SS	6	11	5	10	-	-		1.73
Bischofia javanica	Phyllanthaceae	T	SS	0	0	7	7	-	-		1.67
Melanolepis multiglandulosa	Euphorbiaceae	P	SS	2	1	2	1	-	-		1.67
Ficus erecta var. *beecheyana*	Moraceae	H	SS	4	3	5	4	-	-		1.48
Liquidambar formosana	Altingiaceae	MT	PP	1	1	4	4	-	-		1.45
Sapindus mukorossii	Sapindaceae	MT	SS	2	1	4	3	-	-		1.33
Mallotus japonicus	Euphorbiaceae	H	SS	3	0	4	1	-	-		1.27
Celtis formosana	Cannabaceae	H	SS	0	6	0	6	-	-		1.15
Triadica cochinchinensis	Euphorbiaceae	H	SS	0	3	0	3	-	-		1.05
Broussonetia papyrifera	Moraceae	P	SS	1	2	0	1	-	-		0.88
Cunninghamia konishii	Cupressaceae	MT	PP	20	0	107	87		-		8.39
Prunus campanulata	Rosaceae	H	PP	41	1	77	37		-		5.37
Machilus thunbergii	Lauraceae	MT	SS	12	12	18	18		-		4.02
Cunninghamia konishii	Cupressaceae	MT	PP	15	3	28	16		-		3.28
Idesia polycarpa	Salicaceae	H	SS	7	12	1	6		-		2.60
Acer albopurpurascens	Sapindaceae	T	SS	2	4	3	5		-		2.01
Acer serrulatum	Sapindaceae	H	PP	0	7	1	8		-		1.77
Taiwania cryptomerioides	Cupressaceae	MT	PP	1	0	17	16		-		1.61
Zelkova serrata	Ulmaceae	MT	PP	3	5	1	3		-		1.57
Staphylea formosana	Staphyleaceae	T	SS	1	1	4	4		-		1.39
Calocedrus macrolepis var. *formosana*	Cupressaceae	MT	PP	0	0	2	2		-		1.34

Table 3. *Cont.*

Species Name	Family	Functional Group	SS/PP	HT	PHT	N20	N24	S	W	T	IVI
Ficus fistulosa	Moraceae	H	SS	2	3	1	2		-		1.31
Deutzia pulchra	Hydrangeaceae	T	SS	2	1	2	1		-		1.24
Magnolia compressa	Magnoliaceae	MT	PP	1	5	0	4		-		1.17
Sloanea formosana	Elaeocarpaceae	H	SS	0	2	0	2		-		1.00
Meliosma rhoifolia	Sabiaceae	T	SS	1	2	1	2		-		0.96
Celtis sinensis	Cannabaceae	T	SS	1	1	2	2		-		0.91
Litsea hypophaea	Lauraceae	T	SS	1	1	1	1		-		0.91
Engelhardia roxburghiana	Juglandaceae	H	SS	1	2	0	1		-		0.88
Vernicia montana	Euphorbiaceae	H	SS	1	2	0	1		-		0.71
Diospyros japonica	Ebenaceae	H	SS	0	2	0	2		-		0.63
Lithocarpus amygdalifolius	Fagaceae	T	SS	1	0	3	2		-		0.59
Tetradium glabrifolium	Rutaceae	H	SS	1	2	0	1		-		0.50
Lagerstroemia subcostata	Lythraceae	H	SS	0	1	1	2		-		0.48
Quercus glauca	Fagaceae	T	SS	0	1	0	1		-		0.48
Cinnamomum reticulatum	Lauraceae	MT	SS	0	0	2	2		-		0.48
Reevesia formosana	Malvaceae	T	SS	0	0	2	2		-		0.48
Ficus nervosa	Moraceae	H	SS	0	1	0	1		-		0.46
Castanopsis kawakamii	Fagaceae	T	SS	0	0	1	1		-		0.46
Morus alba	Moraceae	T	SS	0	0	2	2		-		0.45
Alniphyllum pterospermum	Styracaceae	H	SS	0	2	0	2		-		0.45
Daphniphyllum glaucescens subsp. *oldhamii*	Daphniphyllaceae	T	SS	0	0	1	1		-		0.44
Litsea akoensis var. *chitouchiaoensis*	Lauraceae	T	SS	0	0	1	1		-		0.42
Paulownia fortunei	Paulowniaceae	H	SS	1	0	1	0		-		0.42
Bridelia tomentosa	Phyllanthaceae	P	SS	0	1	0	1		-		0.41
Fraxinus griffithii	Oleaceae	MT	SS	0	0	1	1		-		0.41
Eurya strigillosa	Pentaphylacaceae	T	SS	0	0	1	1		-		0.41
Hibiscus taiwanensis	Malvaceae	P	SS	0	1	0	1		-		0.40
Prunus mume	Rosaceae	H	PP	1	1	1	1		-		0.40
Salix fulvopubescens	Salicaceae	H	SS	1	0	1	0		-		0.40
Cryptomeria japonica	Cupressaceae	MT	PP	234	40	1921	1727		-	-	116.13
Chamaecyparis formosensis	Cupressaceae	MT	PP	20	6	292	278		-	-	21.86
Ulmus uyematsui	Ulmaceae	H	SS	5	1	23	19		-	-	3.67
Alnus formosana	Betulaceae	H	SS	8	6	12	10		-	-	3.16
Acer morrisonense	Sapindaceae	H	SS	3	2	8	7		-	-	2.56
Trochodendron aralioides	Trochodendraceae	T	SS	0	2	2	4		-	-	2.24
Chamaecyparis obtusa var. *formosana*	Cupressaceae	MT	PP	0	0	28	28		-	-	1.99
Castanopsis cuspidata var. *carlesii*	Fagaceae	MT	SS	1	0	2	1		-	-	1.83
Pinus taiwanensis	Pinaceae	H	SS	4	0	6	2		-	-	1.73
Machilus japonica	Lauraceae	T	SS	1	1	9	9		-	-	1.37
Castanopsis fargesii	Fagaceae	T	SS	0	0	2	2		-	-	0.94
Carpinus kawakamii	Betulaceae	H	SS	1	0	4	3		-	-	0.92
Pinus armandii	Pinaceae	H	SS	0	0	1	1			-	3.03
Quercus morii	Fagaceae	MT	SS	3	0	8	5			-	1.81
Quercus glandulifera var. *brevipetiolata*	Fagaceae	T	SS	0	0	3	3			-	0.5
Eucalyptus maculata var. *citriodora*	Myrtaceae	MT	PP	0	0	1	1			-	0.42
Eurya loquaiana	Pentaphylacaceae	T	SS	0	0	1	1			-	0.40

In the subtropical zone, non-heliophilous species (MT + T) consist of 14 MT and nine T species; heliophilous species (H + P) consist of 23 H and seven P species. Secondary succession (SS) includes 40 species; Planning Plantation (PP) includes 13 species. In the warm temperate zone, non-heliophilous species comprise 18 MT and 20 T species; heliophilous species comprise 28 H and six P species. SS includes 58 species; PP includes 14 species. In the temperate zone, non-heliophilous species include six MT and five T species; heliophilous species include six H species. SS includes 13 species; PP includes four species (Table 4).

Table 4. Species distribution across the three climate zones was analyzed by functional group and succession regeneration. Climate zone species counts are subtropical (S) = 53; warm temperate (W) = 72; and temperate (T) = 17. Functional group totals are MT (38), T (34), H (57), and P (13). Succession regeneration totals are SS (111) and PP (31).

Variable		S	W	T
Functional Group	MT	14	18	6
	T	9	20	5
	H	23	28	6
	P	7	6	0
Succession Regeneration	SS	40	58	13
	PP	13	14	4
Total		53	72	17

3.1.2. Hazard Tree

The number of hazard trees (HTs) in the temperate (T) zone has exhibited a year-on-year decline, gradually approaching an acceptable level of safety. In contrast, the hazard trees in the subtropical (S) zone have remained stable with a slight increase, while the warm temperate (W) zone has shown a significant upward trend. Overall, the quantity of hazard trees in both the subtropical and warm temperate zones is characterized by a sustained and rising development trajectory.

Regarding the incidence rates within each region, the HT proportion in the temperate (T) zone decreased from 5.8% in 2021 to 0.1% in 2024, while the PHT proportion slightly declined from 0.9% to 0.6%. In the warm temperate (W) zone, the HT proportion remained relatively stable, moving from 7.2% in 2020 to 6.2% in 2024, whereas the PHT proportion rose from 1.2% in 2021 to 3.5% in 2024. In the subtropical (S) zone, the HT proportion increased from 2.9% in 2020 to 8.4% in 2024, and the PHT proportion climbed from 14.9% in 2021 to 25.1% in 2024. These data indicate that the hazard trees in the subtropical and warm temperate zones are continuously intensifying (Table 5).

Table 5. Candidate Inventory and Assessment Tree (CIAT), encompassing both hazard trees (HTs) and Potential Hazard Trees (PHTs), was surveyed across three climate zones.

Period	S			W			T		
	PHT (%)	HT (%)	CIAT	PHT (%)	HT (%)	CIAT	PHT (%)	HT (%)	CIAT
2020	0 (0.0)	6 (2.9)	210	0 (0.0)	118 (7.2)	1628	0 (0.0)	0 (0.0)	1076
2021	32 (14.9)	21 (9.8)	215	17 (1.2)	51 (3.5)	1476	9 (0.9)	59 (5.8)	1026
2022	54 (25.7)	60 (28.6)	210	65 (4.3)	31 (2.1)	1512	14 (1.4)	17 (1.7)	1023
2023	20 (9.6)	21 (10.0)	209	73 (4.9)	91 (6.1)	1495	4 (0.4)	14 (1.4)	1013
2024	63 (25.1)	21 (8.4)	251	51 (3.5)	87 (6.2)	1459	6 (0.6)	1 (0.1)	1018

3.2. HT/PHT Correlation

A significant, positive correlation (r = 0.54) exists between hazard tree (HT) and Potential Hazard Tree (PHT) incidences. The test statistic (t = 4.1245, $p < 0.00017$) confirms a significant association between the variables. The 95% confidence interval (0.286, 0.719), which excludes zero, further validates the robustness of this positive relationship. A higher PHT incidence within an area corresponds to an increased HT incidence, demonstrating a consistent trend.

3.3. Hazard Tree Model

Model reference level—functional group = H + P (heliophilous), succession regeneration = PP (Planning Plantation), and climate zone = temperate zone.

HT incidence analysis indicates the order of factor influence—climate zone (S ≈ W > T); succession regeneration (SS > PP); and functional group (H + P > MT + T).

$$\begin{aligned}(HT\ Ratio) = 5.97 &- 0.28(Functional\ Group - MT + T) \\ &+ 1.90(Succession\ Regeneration - SS) \\ &+ 1.93(Climate\ Zone - W) + 1.96(Climate\ Zone - S)\end{aligned} \quad (6)$$

All three factors reached a level of high statistical significance ($p < 0.001$) for HT incidence, confirming the predictive robustness of the model (Table 6). According to the absolute values of the estimates, the relative influence of the factors followed the order functional group > climate zone ≈ succession type. The exponentiated coefficients, expressed as Incidence Rate Ratios (IRRs), quantified the specific impact of each factor:

Table 6. Hazard tree model metrics.

Variable	Estimate	*p*-Value	Exponentiated Coefficients
Intercept	1.79	$<2 \times 10^{-16}$	5.97
Functional Group			
MT + T	−1.29	$<2 \times 10^{-16}$	0.28
Succession Regeneration			
SS	0.64	7.4×10^{-11}	1.90
Climate Zone			
W	0.66	8.8×10^{-7}	1.93
S	0.67	4.7×10^{-7}	1.96

Functional Group: Compared to the heliophilous (H + P) reference group, the non-heliophilous (MT + T) group exhibited an HT incidence ratio 0.28 times that of the control.

Succession Type: Compared to the Planning Plantation (PP) reference group, the HT incidence ratio of secondary succession (SS) was 1.90 times higher.

Climate Zone: Compared to the temperate (T) reference group, the HT incidence ratio was 1.93 times higher in the warm temperate (W) zone and 1.96 times higher in the subtropical (S) zone (Table 6).

3.4. Potential Hazard Tree Model

All three factors reached a level of high statistical significance ($p < 0.001$) for PHT incidence, confirming the predictive robustness of the model. According to the absolute values of the estimates, the relative influence of the factors followed the order climate zone > succession type > functional group. The exponentiated coefficients, expressed as Incidence Rate Ratios (IRRs), quantified the specific impact of each factor (Table 7).

Functional Group: Compared to the heliophilous (H + P) reference group, the non-heliophilous (MT + T) group exhibited a PHT incidence ratio 0.32 times that of the control.

Succession Type: Compared to the Planning Plantation (PP) reference group, the PHT incidence ratio of secondary succession (SS) was 4.47 times higher.

Climate Zone: Compared to the temperate (T) reference group, the PHT incidence rate was 8.13 times higher in the warm temperate (W) zone and 11.46 times higher in the subtropical (S) zone.

Table 7. Potential hazard tree model metrics.

Variable	Estimate	*p*-Value	Exponentiated Coefficients
Intercept	−0.30	0.26	0.74
Functional Group			
MT + T	−1.14	$<2 \times 10^{-16}$	0.32
Succession Regeneration			
SS	1.50	$<2 \times 10^{-16}$	4.47
Climate Zone			
W	2.10	$<2 \times 10^{-16}$	8.13
S	2.44	$<2 \times 10^{-16}$	11.46

Both models confirmed that climate zone (S/W), succession type (SS), and functional group (H + P) are significant factors increasing the incidence of both HT and PHT (Table 7).

$$\begin{aligned}(PHT\ Ratio) = \ & 0.74 + 0.32(Functional\ Group - MT + T) \\ & + 4.47(Succession\ Regeneration - SS) \\ & + 8.13(Climate\ Zone - W) + 11.4(Climate\ Zone - S)\end{aligned} \quad (7)$$

HT incidence analysis indicates the order of factor influence—climate zone (S > W > T); succession regeneration (SS > PP); and functional group (H + P > MT + T).

3.5. Prediction of Hazard Tree Occurrence Ratio

Incidence ratios of HT and PHT are significantly concentrated within the subtropical (S) and warm temperate (W) zones. HT/PHT incidence in the temperate (T) zones remained consistently low. The S and W zones exhibited high volatility and sustained contributions. The persistent incidence from these high-ratio zones offset the stability of the temperate zones, resulting in the failure of the overall incidence ratio to improve.

The established model was utilized to predict HT and PHT incidence ratio across all 12 factor combinations (functional group + succession regeneration + climate zone, FSC). The one-sample *t*-test results indicated a mean predicted HT incidence of 8.97% ($p < 0.001$; highly significant) and a mean predicted PHT incidence of 9.19% ($p < 0.01$; significant). These results reveal that incidence ratios are driven by significant disparities arising from a few extreme high-incidence combinations. The highest incidence ratios were consistently observed in FSC 1 ((H + P) + SS + S) and FSC 2 ((H + P) + SS + W), dashed line exhibit this phenomenon. The lowest incidence ratios were consistently found in FSC 12 ((MT + T) + PP + T). The functional group is the most critical factor influencing HT incidence. The incidence ratios for all heliophilous (H + P) combinations (FSC 1–6) consistently exceeded those of all non-heliophilous (MT + T) combinations (FSC 7–12). Succession type serves as the secondary influencing factor, where the incidence of secondary succession (SS) consistently surpassed that of Planning Plantation (PP) (e.g., FSC 1 > FSC 4; FSC 7 > FSC 10). Climate zone was found to have the least impact on HT incidence (Figure 3).

Climate zone is the most critical factor influencing PHT incidence. Under identical combinations of functional groups and succession types (e.g., FSC 1–3, FSC 4–6, FSC 7–9, and FSC 10–12), a consistent trend of S > W > T was observed. Succession type serves as the secondary influencing factor, with the incidence of secondary succession (SS) consistently surpassing that of Planning Plantation (PP) (e.g., FSC 1 > FSC 4; FSC 7 > FSC 10). While the incidence ratios of all heliophilous (H + P) combinations (FSC 1–6) exceeded those of all

non-heliophilous (MT + T) combinations (FSC 7–12), the functional group exhibited the least overall effect within the PHT model (Figure 3).

FSC1 = (H + P) + SS + S, FSC2 = (H + P) + SS + W, FSC3 = (H + P) + SS +T; FSC4 = (H + P) + PP + S, FSC5 = (H + P) + PP + W, FSC6 = (H + P) + PP + T; FSC7 = (MT + T) + SS + S, FSC8 = (MT + T) + SS + W, FSC9 = (MT + T) + SS +T; FSC10 = (MT + T) + PP + S, FSC11 = (MT + T) + PP + W, FSC12 = (MT + T) + PP + T.

The predicted distribution of incidence ratios exhibited statistical significance (PHT: $p < 0.001$; HT: $p < 0.05$). These incidence ratios are primarily driven by the intense influence of a few specific combinations of high-incidence factors. A clear gradient distribution is evident, where a dashed line delineates the factor combinations into two groups. The highest HT and PHT incidence occurs under the (H + P) + SS + S/W combinations. The lowest incidence is consistently found under the (MT + T) + PP+ T combination. Factor influence weight ranking is: functional group > succession regeneration > climate zone.

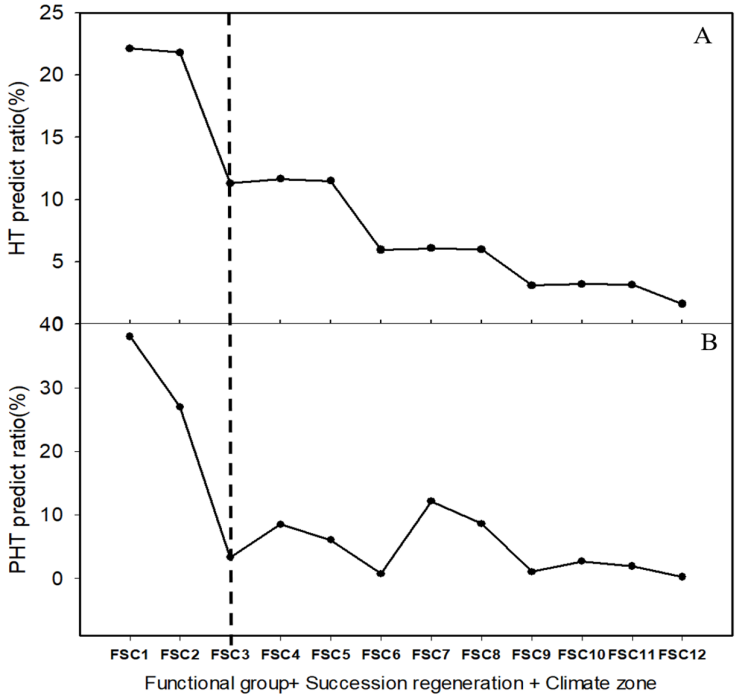


Figure 3. Prediction model (functional group + succession regeneration + climate zone, FSC) and HT and PHT incidence ratios. (**A**) HT prediction model; (**B**) PHT prediction model.

4. Discussion

Over the five-year period (2020–2024), the overall incidence of hazard trees (HTs) and Potential Hazard Trees (PHTs) along the Alishan Forest Railway corridor has not improved to an acceptable level of safety. This persistent high incidence is not attributable to stochasticity but is driven by the continuous contribution of specific climate zones. PHT identification is primarily based on standardized health and structural assessments [3,4,25–32]. Consequently, the model results reflect characteristics dominated by environmental context. Climate zone exerts the greatest influence, followed by succession, while functional group receives the lowest weight.

In contrast, the HT model indicates that functional group is the most critical factor, with incidence ratios exhibiting a clear stratification (FSC 1–6 > FSC 7–12), highlighting the divergence between heliophilous (H + P) and non-heliophilous (MT + T)

species. Many heliophilous species, characterized by rapid growth and lower resistance, may undergo sudden failure (developing into HT) due to climatic conditions even before reaching PHT thresholds in standardized assessments. Conversely, while non-heliophilous (MT + T) species may be identified as PHT due to structural defects, their inherent growth characteristics render them less prone to transforming into actual HT under environmental stress.

The high incidence in the subtropical (S) and warm temperate (W) zones primarily stems from the combination of heliophilous species (H + P) and secondary succession (SS). The failure to reduce incidence ratios over the five-year period results from the continuous recruitment of high-incidence heliophilous species via secondary succession within these zones. These climate zones, characterized by high species richness and diversity [11–13], provide a more abundant "invasion pool" for high-incidence heliophilous species [39], encompassing the majority of species belonging to the H + P and SS combination.

4.1. Structural Defects Relative Frequency

4.1.1. Whole Tree Structure—D1 (Lean)

Statistical analysis of HT and PHT structural defect percentages (Table 8) shows that structural defects impact H + P species significantly more than MT + T species, with HT defects reaching significance ($p < 0.03$) and PHT defects showing non-significance ($p < 0.06$). The D1 structural defect is significantly associated with increased incidence ratios in H + P species (HT-26.1%; PHT-37.2%), but it is notably less significant for MT + T species (PHT-1.5%; HT-0.8%) (Table 8). This disparity is linked to the H + P species' "fast growth" strategy [40] and their poor "postural control" and "self-support". Due to the corridor's persistent light environment, H + P species exhibit strong phototropism toward the open railway space, resulting in stem lean. Their inferior "postural control" and "self-support" subsequently increase the likelihood of failure. Conversely, MT + T species exhibit slower growth but possess superior "postural control" and "self-support" compared to H + P species [40,41], thus resulting in a lower D1 failure potential. Consistent with [41], H + P species demonstrated poorer performance in both postural control and self-support relative to MT + T species.

Table 8. HT and PHT relative frequency percentage of structural defects (2020–2024). * D1 = lean; D2 = root decay issues; D3 = root structural defects; D4 = root plate soil separation; D5 = trunk base decay; D6 = over-extended branches; D7 = co-dominant stems; D8 = scaffold branch decay; D9 = growth decline or deadwood. Analysis indicates statistical significance for HT ($p < 0.03$) and a marginal trend for PHT ($p < 0.06$). The results show that for HT, D1, D3, D5, and D9 frequencies are higher in H + P than in MT + T (H + P > MT + T). The PHT results similarly show H + P > MT + T for D1 and D3.

Variable	Functional Group	Tree Structural Defects (%) *									*p*-Value	Mean Comparison
		D1	D2	D3	D4	D5	D6	D7	D8	D9		
HT	H + P	26.1	1.5	23.5	4.4	14.4	5.7	0.9	0.7	8.9	0.03	H + P > MT + T
	MT + T	0.8	0.9	0.7	3.2	1.9	0.3	0.2	0.1	7.0		
PHT	H + P	37.2	1.1	20.3	2.7	3.1	9.1	3.8	0.9	4.6	0.06	H + P > MT + T
	MT + T	1.5	0.1	1.2	2.1	2.7	0.6	0.3	0.0	0.9		

4.1.2. Root Structure—D2 (Root Decay), D3 (Root Structural Defects), D4 (Root Plate Soil Separation)

D3 significantly impacts H + P species failure potential (HT-23.5%; PHT-20.3%) but not MT + T species (HT-0.7%; PHT-1.2%). Development, engineering disturbances, and climatic impacts within the railway corridor drive slope soil erosion and sliding [42,43]. The

root structure of H + P tree species is constrained by soil volume and affected by adverse water dynamics [44,45], which can easily lead to structural defects or expose structural roots, thereby increasing the likelihood of tree collapse [46]. This susceptibility reflects H + P species' low tolerance and poor TNC [40,47], rendering roots unable to cope with environmental dynamics; combined with inherently poor root structural stability, these factors amplify D3 failure potential. MT + T species possess a higher root/stem biomass ratio (MT + T > H + P), where their growth strategy confers superior tolerance, TNC, and structural stability [9].

D4 proved insignificant for both H + P and MT + T species, though the impact on H + P species (HT: 4.4%; PHT: 2.7%) was slightly higher than on MT + T species (HT-3.2%; PHT-2.1%). The Potential Impact Zone (PIZ) for trees on steep slopes (>15°) may expand beyond 1.5 times the tree height [48]. H + P species, driven by high light demand, prioritize colonization of these eroded, exposed slopes. Frequent soil erosion and slope sliding within the railway corridor compromise the stability between the soil and the root plate, thereby increasing H + P failure potential.

4.1.3. Trunk Base—D5 (Trunk Base Decay)

D5 influence on PHT failure potential was insignificant for both H + P (2.7%) and MT + T (2.1%) species. In HT, D5 significantly influenced H + P failure potential (14.4%), creating a marked difference from MT + T species (1.9%) (Table 8). The low defense, low storage strategy of H + P species results in insufficient energy to resist fungal invasion, thereby predisposing trunk bases to decay [33,47].

MT + T species prioritize energy investment in defense, storage, and robust underground structural development. Higher tolerance and TNC defense against invasion ensure superior trunk base structural stability, reducing failure potential.

4.1.4. Scaffold Branches—D6 (Over-Extended Branches), D7 (Co-Dominant Stems), D8 (Scaffold Branch Decay)

D6 significantly impacted H + P species (HT-5.7%; PHT-9.1%) compared to MT + T species (HT-0.3%; PHT-0.6%) (Table 8). This pattern correlates with the H + P "fast growth" strategy. Competition for abundant sunlight within the railway corridor drives continuous branch growth toward the opening, resulting in over-extension and canopy imbalance. H + P species, characterized by poor "postural control" and "self-support," fail to regulate their geometry, thereby increasing failure potential. Conversely, MT + T species, possessing superior "postural control" and "self-support" [41], mitigate excessive extension and branch failure issues [49].

D7 influence on failure potential was relatively insignificant for both H + P species (PHT-3.8%; HT-0.9%) and MT + T species (PHT-0.3%; HT-0.2%). This result suggests that co-dominant stems are not a primary driver of tree failure; however, they may amplify the severity of other structural defects, such as D1 and D6.

D8 influence on failure potential was similarly insignificant for H + P species (PHT-0.9%; HT-0.7%) and MT + T species (PHT-0.0%; HT-0.1%). This outcome suggests that scaffold branches are less exposed to railway corridor adversity and disturbance; consequently, mechanical damage and decay resulting from engineering operations are minimal.

4.1.5. Tree Biological Vitality—D9 (Growth Decline or Deadwood)

The D9 results indicate a significant impact on H + P species (PHT-4.6%; HT-8.9%) compared to MT + T species (PHT-0.9%; HT-7.0%); H + P species are notably more prone to decline and mortality (Table 8). Regarding life span, H + P species are generally shorter-lived than MT + T species (H + P < MT + T). The "fast growth" strategy restricted defense and storage, resulting in lower stress tolerance and TNC (H + P < MT + T); consequently,

H + P species are more susceptible to growth decline and mortality [47]. D9 also significantly impacts MT + T species within the HT category (7.0%). Observed decline and mortality in these trees are attributable to drastic environmental changes or disturbances along the railway corridor, such as root severance during engineering or ballast covering the tree base.

4.2. Functional Group—H + P > MT + T

Compared to non-heliophilous (MT + T) species, heliophilous (H + P) species exhibit a significantly higher incidence of HT/PHT, driven by their short life cycle strategy characterized by "high recruitment, rapid growth, high mortality, and short lifespan" [8,9]. H + P species prioritize resource allocation toward growth and reproduction, enhancing their recruitment capacity at the expense of defense, storage, longevity, and resprouting ability [40]. This strategy results in critical biomechanical vulnerabilities: low stress tolerance, limited total non-structural carbohydrate (TNC) reserves [40,50], and a lower root-to-shoot biomass ratio [9]. As TNC is a crucial energy reserve for stress response and the compartmentalization of decay, H + P species lack sufficient bioenergy to maintain root structural integrity when facing corridor slope erosion or fungal invasion. Consequently, their roots and buttresses are highly susceptible to lethal defects, such as aggressive root diseases, root rot, or basal rot, as well as root hollowing or fracture [32] (Table 8), leading to high mortality and high hazard tree incidence.

In contrast, MT + T species adopt a long life cycle strategy defined by slow growth, low recruitment, low mortality, and long lifespans. Their growth strategy prioritizes conservative resource allocation toward defense and storage to develop stable underground structures [40,50]. Their high TNC storage, robust resprouting ability, and high root-to-shoot biomass ratio [9] contribute to superior structural stability and lower mortality ratios, significantly reducing the probability of evolving into hazard trees. This is supported by our 2020–2024 structural defect analysis, which reveals that structural defects (D1–D8) are rarely the primary cause of failure in MT + T species. Instead, MT + T hazard trees (n = 193) predominantly exhibit growth decline or standing deadwood issues (D9). This indicates that the failure potential of MT + T species is not driven by intrinsic biomechanical instability but rather reflects natural physiological senescence during the mature or aging phases of their life cycle (Table 8).

4.3. Succession Regeneration—SS > PP

Succession and recruitment are primarily driven by the seed bank and seed rain [47]. Continuous slope erosion and disturbances create bare ground, where secondary succession (SS) within the railway corridor favors the colonization of high-recruitment heliophilous (H + P) species. Once these H + P species establish themselves as mother trees, they generate a dominant seed bank in the area. Consequently, when subsequent disturbances occur, the exposed soil is immediately recolonized by the H + P seed bank, creating a feedback loop of "SS → H + P → H + P Seed Bank → SS." This cycle traps the succession in a stem exclusion phase dominated by heliophilous species competition and exclusion.

In contrast, Planning Plantation (PP) consists of anthropogenically selected non-heliophilous (MT + T) species (*Cryptomeria japonica*, *Chamaecyparis formosensis*), which serve as the primary mother trees. Their seed banks are naturally dominated by MT + T species. Thus, despite sufficient light in newly formed canopy gaps, the lack of H + P seed input results in these gaps being occupied by stable MT + T progeny. This maintains a stable "PP → MT + T → MT + T Seed Bank → PP" cycle, leading to an Understory Reinitiation Phase or a stable Climax Phase dominated by non-heliophilous species.

4.4. Climate Zone—S ≈ W > T

Variations in sunlight duration drive species diversity differences across climate zones. The subtropical (S) and warm temperate (W) zones (elevation 50–1711 m), influenced by elevation and topography, benefit from longer sunlight duration, where sufficient light fosters the highest species richness and diversity (Tables 2 and 5). This light environment concentrates the majority of heliophilous (H + P) species within these zones (subtropical: 30; warm temperate: 34). Conversely, the high-altitude temperate zone (T) (1711–2405 m), characterized by short sunlight duration and harsh environmental conditions, fails to meet the growth requirements of heliophilous species, limiting species growth and distribution; this constraint results in significantly reduced species richness and diversity and a simplified vegetation structure [13]. Temperate H + P species number only 6 has no pioneer (P) species. Sunlight duration across climate zones determines the size of the heliophilous species pool, subsequently affecting the incidence ratio within the corridor (Table 4).

5. Conclusions

The persistently high incidence of hazard trees (HTs) along the railway corridor stems from environmental characteristics defined by long-term light exposure and slope erosion. These continuous chronic disturbances create bare ground, driving secondary succession (SS) dominated by heliophilous (H + P) species. Once established, H + P species serve as dominant mother trees, providing a continuous seed source for newly disturbed sites via the seed bank, thereby forming a self-reinforcing cycle. Adopting a short life cycle strategy (characterized by high mortality and short lifespans), H + P species are highly susceptible to stem lean (D1) and root structural defects (D3) in sloped environments. Under sudden and rapid pulse disturbances [51], such as extreme weather events, these species rapidly develop into hazard trees and undergo failure. In contrast, Planning Plantations (PPs) in the temperate (T) zone, composed of non-heliophilous (MT + T) species, leverage their stable growth strategies and biomechanical resilience as seed sources to inhibit H + P recruitment, effectively maintaining HT/PHT incidence at minimum levels.

The divergence between HT and PHT models in response to influencing factors reveals the limitations of current hazard tree identification assessment standards. While actual tree failure (HT) is heavily influenced by the functional traits of the species, current PHT identification relies on standardized health and structural scoring. This system focuses on the external manifestation of physical defects while overlooking the "tolerance" and "resilience" inherent to different functional groups. Consequently, the PHT model is most heavily weighted by climate zone context, while functional group importance is minimized. Future hazard tree identification along forest railways should incorporate functional group weighting into the scoring system to correct the systematic underestimation in heliophilous species and the overestimation of structural defects in non-heliophilous species.

Hazard tree management strategies must shift from "reactive removal" to "proactive stand improvement." In the subtropical (S) and warm temperate (W) zones, Planning Plantations (PPs) should prioritize native non-heliophilous (MT + T) species that match local climatic conditions and ecological amplitudes. Strategically utilizing MT + T species to replace H + P species will accelerate the transition of the railway corridor from the stem exclusion phase toward stable "understory reinitiation" and "climax phase" stages. This will fundamentally reduce HT/PHT incidence in subtropical and warm temperate zones, ensuring the long-term operational safety of the forest railway corridor.

Author Contributions: Conceptualization, M.-H.C.; methodology, M.-H.C. and J.-T.L.; validation, M.-H.C., J.-T.L. and P.-J.C.; formal analysis, M.-H.C. and J.-T.L.; investigation, M.-H.C. and P.-J.C.; resources, M.-H.C.; data curation, M.-H.C. and P.-J.C.; writing—original draft preparation, M.-H.C.

and P.-J.C.; writing—review and editing, M.-H.C. and J.-T.L.; visualization, M.-H.C. and J.-T.L.; supervision, M.-H.C. and J.-T.L.; project administration, M.-H.C.; funding acquisition, M.-H.C. All authors have read and agreed to the published version of the manuscript.

Funding: This research was supported by the Alishan Forest Railway and Cultural Heritage Office, Forestry and Nature Conservation Agency, Taiwan, under the "Research Plan for Tree Structural Safety and Risk Management along the Alishan Forest Railway (2019–2022)", funding number: 108TM-MA-8, 111TA-MM-103, 112TA-MM-103, and the "Research Plan for Tree Safety Management along the Alishan Forest Railway (2025–2027)", funding number: 114TA-MM-103.

Data Availability Statement: The data presented in this study are available in the Table 3.

Acknowledgments: The authors wish to thank the Alishan Forest Railway and Cultural Heritage Office, Forestry and Nature Conservation Agency, Ministry of Agriculture, Taiwan, for its support and assistance during the field investigation and data collection. The authors have reviewed and edited the output and take full responsibility for the content of this publication.

Conflicts of Interest: The authors declare no conflicts of interest.

References

1. Control Yuan. *Investigation Report on the Derailment Incident of the Alishan Forest Railway on 27 April 2011*; Case No. 100NEWS014; Control Yuan: Taipei, Taiwan, 2011.
2. Tree Care Industry Association. *ANSI A300 (Part 9)-2011: Tree, Shrub, and Other Woody Plant Management—Standard Practices (Tree Risk Assessment a. Tree Structure Assessment)*; Tree Care Industry Association, Inc.: Londonderry, NH, USA, 2011.
3. Angwin, P.A.; Cluck, D.R.; Zambino, P.J.; Oblinger, B.; Woodruff, W.C. *Hazard Tree Guidelines for Forest Service Facilities and Roads in the Pacific Southwest Region*; Report No. RO-12-01; U.S. Department of Agriculture, Forest Service, Pacific Southwest Region, Forest Health Protection: Vallejo, CA, USA, 2012.
4. Gooding, R.F.; Clark, J.R.; Severynen, P.; Vicary, B.P.; Duntemann, M.; Burkhart, L.; Smiley, E.T. *Guide for Plant Appraisal*, 10th ed.; International Society of Arboriculture: Atlanta, GA, USA, 2019.
5. Smiley, E.T.; Fraedrich, B.R. Determining strength loss from decay. *J. Arboric.* **1992**, *18*, 201–204. [CrossRef]
6. Johnstone, D.; Moore, G.; Tausz, M.; Nicolas, M. The measurement of wood decay in landscape trees. *Arboric. Urban For.* **2010**, *36*, 121–127. [CrossRef]
7. Blodgett, J.T.; Burns, K.S.; Lalande, B.M. *Hazard Tree Management*; Technical Report R2-73; U.S. Department of Agriculture, Forest Service, Rocky Mountain Region, Forest Health Protection: Lakewood, CO, USA, 2021.
8. Wright, S.J.; Muller-Landau, H.C.; Condit, R.; Hubbell, S.P. Gap-dependent recruitment, realized vital rates, and size distributions of tropical trees. *Ecology* **2003**, *84*, 3174–3185. [CrossRef]
9. Poorter, L.; Bongers, L.; Bongers, F. Architecture of 54 moist-forest tree species: Traits, trade-offs, and Functional Groups. *Ecology* **2006**, *87*, 1289–1301. [CrossRef]
10. Delcamp, M.; Gourlet-Fleury, S.; Flores, O.; Garnier, E. Can functional classification of tropical trees predict population dynamics after disturbance. *J. Ecol.* **2008**, *96*, 236–247. [CrossRef]
11. Su, H.J. Studies on the climate and vegetation types of the natural forests in Taiwan (1): Analysis of the variations in climatic factors. *Q. J. Chin. For.* **1984**, *17*, 1–14.
12. Su, H.-J. Studies on the climate and vegetation type of the natural forest in Taiwan. II. Altitudinal vegetation zones in relation to temperature gradient. *Q. J. Chin. For.* **1984**, *17*, 57–73.
13. Hsieh, C.F. Composition, endemism and phytogeographical affinities of the Taiwanese flora. *Taiwania* **2002**, *47*, 298–310.
14. Körner, C. The use of 'altitude' in ecological research. *Trends Ecol. Evol.* **2007**, *22*, 569–574. [CrossRef]
15. Oliver, C.D.; Larson, B.C. *Forest Stand Dynamics*; John Wiley & Sons: New York, NY, USA, 1996.
16. Su, H.J. Ten years for trees, a century for forest: Illustration of forest vegetation succession. *For. Res. Newsl.* **2014**, *21*, 1–8.
17. Harris, R.W.; Clark, J.R.; Matheny, N.P. *Arboriculture: Integrated Management of Landscape Trees, Shrubs, and Vines*, 4th ed.; Prentice Hall: Upper Saddle River, NJ, USA, 2004.
18. Paquette, A.; Messier, C. The effect of biodiversity on tree productivity: From temperate to boreal forests. *Glob. Ecol. Biogeogr.* **2010**, *19*, 693–704. [CrossRef]
19. Lavorel, S.; McIntyre, S.; Landsberg, J.; Forbes, T.D.A. Plant functional classifications: From general groups to specific groups based on response to disturbance. *Trends Ecol. Evol.* **1997**, *12*, 474–478. [CrossRef] [PubMed]

20. Curtis, J.T.; McIntosh, R.P. An upland forest continuum in the prairie-forest border region of Wisconsin. *Ecology* **1951**, *32*, 476–496. [CrossRef]
21. Shannon, C.E.; Weaver, W. *The Mathematical Theory of Communication*; University of Illinois Press: Urbana, IL, USA, 1949.
22. Simpson, E.H. Measurement of diversity. *Nature* **1949**, *163*, 688. [CrossRef]
23. Alatalo, R.V. Problems in the measurement of evenness in ecology. *Oikos* **1981**, *37*, 199–204. [CrossRef]
24. Hill, M.O. Diversity and evenness: A unifying notation and its consequences. *Ecology* **1973**, *54*, 427–432. [CrossRef]
25. Mattheck, C.; Breloer, H. *The Body Language of Trees*; The Stationery Office: London, UK, 1994.
26. Hickman, G.W.; Perry, E.; Evans, R. Validation of a tree failure evaluation system. *J. Arboric.* **1995**, *21*, 233–234. [CrossRef]
27. Wassenaer, P.; Richardson, M. A review of tree risk assessment using minimally invasive technologies and two case studies. *Arboric. J.* **2009**, *32*, 275–292. [CrossRef]
28. Hayes, E. Tree risk assessment and tree mechanics. *Arboric. Urban For.* **2002**, *7*, 33–37. [CrossRef]
29. Trummer, L.; Hennon, P. *Hazard Trees in Alaska: A Guide to the Identification and Management of Hazard Trees in Alaska*; U.S. Department of Agriculture, Forest Service, Pacific Southwest Region, Forest Health Protection: Vallejo, CA, USA, 2009.
30. Filip, G.M.; Biro, J.; Chadwick, K.L.; Goheen, D.J.; Goheen, E.M.; Hadfield, J.S. *Field Guide for Hazard-Tree Identification and Mitigation on Developed Sites in Oregon and Washington Forests*; Report No. R6-NR-TP-021-2013; U.S. Department of Agriculture, Forest Service, Pacific Northwest Region, Forest Health Protection: Portland, OR, USA, 2014.
31. Filip, G.; Barger, M.; Bronson, J.; Chadwick, K.; Collins, R.; Goodrich, B.; Kearns, H.; McWilliams, M.; Oblinger, B.; Omdal, D.; et al. *Field Guide for Danger-Tree Identification and Response Along Forest Roads and Work Sites in Oregon and Washington*; U.S. Department of Agriculture, Forest Service, Pacific Southwest Region, Forest Health Protection: Vallejo, CA, USA, 2016.
32. Guyon, J.; Cleaver, C.; Jackson, M.; Saavedra, A.; Zambino, P. *A Guide to Identifying, Assessing, and Managing Hazard Trees in Developed Recreational Sites of the Northern Rocky Mountains and the Intermountain West*; Report No. R1-17-31; U.S. Department of Agriculture, Forest Service, State and Private Forestry, Northern and Intermountain Regions: Missoula, MT, USA, 2017.
33. Angwin, P.A.; Cluck, D.R.; Rosen, J.; Woodruff, W.C.; Hawkins, A.E.; Barnes, C.W.; Cannon, P.G.; Hazelhurst, S. *Hazard Tree Identification and Mitigation*; FHP Report No. RO-22-01; U.S. Department of Agriculture, Forest Service, Pacific Southwest Region, Forest Health Protection: Vallejo, CA, USA, 2022.
34. Kuo, Y.-L.; Lin, T.-Y.; Yang, Y.-Y.; Chen, H.-L.; Yang, C.-K.; Yu, S.-Y. Photosynthetic Characteristics and Shade Tolerance of 440 Native Woody Species in Taiwan. *Taiwan J. For. Sci.* **2021**, *36*, 189–220.
35. Zhang, D.; Stanturf, J.A. Forest Plantations. In *Encyclopedia of Ecology*; Jørgensen, S.E., Fath, B.D., Eds.; Elsevier: Oxford, UK, 2008; Volume 5, pp. 1673–1680.
36. Nelder, J.A.; Wedderburn, R.W.M. Generalized linear models. *J. R. Stat. Soc. Ser. A* **1972**, *135*, 370–384. [CrossRef]
37. Zuur, A.F.; Ieno, E.N.; Walker, N.J.; Saveliev, N.J.; Smith, G.M. *Mixed Effects Models and Extensions in Ecology with R*; Springer: New York, NY, USA, 2009.
38. McCullagh, P.; Nelder, J.A. *Generalized Linear Models*, 2nd ed.; Chapman & Hall/CRC: Boca Raton, FL, USA, 1989.
39. Chazdon, R.L. *Second Growth: The Promise of Tropical Forest Regeneration in an Age of Deforestation*; University of Chicago Press: Chicago, IL, USA, 2014.
40. Poorter, L.; Kitajima, K. Carbohydrate storage and light requirements of tropical moist and dry forest tree species. *Ecology* **2007**, *88*, 1000–1011. [CrossRef] [PubMed]
41. Fournier, M.; Dlouhá, J.; Jaouen, G.; Almeras, T. Integrative biomechanics for tree ecology: Beyond wood density and strength. *J. Exp. Bot.* **2013**, *64*, 4793–4815. [CrossRef] [PubMed]
42. Miller, K.F. *Windthrow Hazard Classification; Leaflet 85*; Forestry Commission: Edinburgh, UK, 1985; pp. 1–17. Available online: https://cdn.forestresearch.gov.uk/1985/04/fclf085_1985.pdf (accessed on 9 March 2026).
43. Hauer, R.J.; Wang, W.; Dawson, J.O. Ice storm damage to urban trees. *J. Arboric.* **1993**, *19*, 187–194. [CrossRef]
44. Lindsey, P.; Bassuk, N.L. Specifying soil volumes to meet the water needs of mature urban street trees and trees in containers. *J. Arboric.* **1991**, *17*, 141–148. [CrossRef]
45. Nielsen, C.N.; Bühler, O.; Kristoffersen, P. Soil water dynamics and growth of street and park trees. *Arboric. Urban For.* **2007**, *33*, 231–245. [CrossRef]
46. Jim, C.Y.; Zhang, H. Defect-disorder and risk assessment of heritage trees in urban Hong Kong. *Urban For. Urban Green.* **2013**, *12*, 585–596. [CrossRef]
47. Guariguata, M.R.; Ostertag, R. Neotropical secondary forest succession: Changes in structural and functional characteristics. *For. Ecol. Manag.* **2001**, *148*, 185–206. [CrossRef]
48. Whilhelmi, N.P.; Reynolds, G.J. *Tree Risk Assessment and Hazard Tree Mitigation in the Southwestern Region*; Report No. TP-R3-16-37; U.S. Department of Agriculture, Forest Service, Southwestern Region, Forest Health Protection: Albuquerque, NM, USA, 2024.
49. Bellingham, P.J.; Sparrow, A.D. Multi-stemmed trees in montane rain forests: Their frequency and demography in relation to elevation, soil nutrients and disturbance. *J. Ecol.* **2009**, *97*, 472–483. [CrossRef]

50. Myers, J.; Kitajima, K. Carbohydrate storage enhances seedling shade and stress tolerance in a neotropical forest. *J. Ecol.* **2007**, *95*, 383–395. [CrossRef]
51. Lundquist, J.E.; Camp, A.E.; Tyrrell, M.L.; Seybold, S.J.; Cannon, P.; Lodge, D.J. Earth, wind, and fire: Abiotic factors and the impacts of global environmental change on forest health. In *Forest Health: An Integrated Perspective*, 1st ed.; Castello, J.D., Teale, S.A., Eds.; Cambridge University Press: Cambridge, UK, 2011; pp. 195–243.

Disclaimer/Publisher's Note: The statements, opinions and data contained in all publications are solely those of the individual author(s) and contributor(s) and not of MDPI and/or the editor(s). MDPI and/or the editor(s) disclaim responsibility for any injury to people or property resulting from any ideas, methods, instructions or products referred to in the content.